Available online at www.sciencedirect.com
ScienceDirect
Scripta Materialia 58 (2008) 372–376
Scripta MATERIALIA
www.elsevier.com/locate/scriptamat

Viewpoint Paper

A flow-partitioned deformation zone model for defect formation during friction stir welding

William J. Arbegast

NSF Center for Friction Stir Processing, Advanced Materials Processing and Joining Center, South Dakota School of Mines and Technology, Rapid City, SD 57701, USA

Received 31 July 2007; revised 30 September 2007; accepted 18 October 2007

Abstract—A friction stir welding (FSW) metalworking model is proposed which partitions flow through distinct deformation zone geometries around the pin probe and beneath the shoulder. These geometries form under the effects of the temperature field, constitutive properties, strain rate and pin tool geometry in these zones. Inadequacies in this flow are related to specific FSW defect types. An initial volume of material equal to the projected area of the pin tool probe is assumed to enter the FSW processing zone. An excess material function is presented in terms of controllable process parameters to describe flowing material added to this initial volume due to temperature and pressure conditions around the pin tool. A forcing function defines the state of applied stresses which partitions the flow through these distinct zones to fill the cavity behind the pin tool. These are equated using the equations of motion for a multi-body dynamic system. Only the concept of a flow-partitioned deformation zone model is presented in this paper. Experimental validation of the model is in progress and the results will be made available in the future.

Keywords: Friction stir welding; Defects; Deformation zones; Flow partitioning; Mass balance

1. Introduction

Significant advances have been made in friction stir welding (FSW) technology over the last 15 years [1]. An excellent review of the state of the art has been given by Mishra and Ma [2]. FSW has been described as a solid-state metalworking process with flow progressing through sequential pre-heat, initial deformation, extrusion, forging and cool-down metallurgical processing zones [3]. Within the extrusion zone, periodic, finite width, wiping flow patterns form beneath the shoulder and around the probe (Fig. 1). Leading-edge initial deformation zone material defined by the projected area of the probe flows through the extrusion zone to converge and consolidate in the trailing-edge forging zone. "Excess" flowing material is added to the initial projected area of the probe within the extrusion zone based on tool design, flow stress, temperature and processing parameters. It is interesting to note that these flow zones and patterns are observed in all metallic and thermoplastic material FSW – with only the volume and direction of material wiping through each zone differing.

Colegrove et al. [4] have shown by numerical simulation that the interaction of the temperature field, constitutive properties and strain rate conditions governs the extent of metal flow beneath the shoulder and adjacent to the probe. Schmidt and Hattel [5] have shown a confined shear flow region forming immediately adjacent to the pin probe, bounded by a critical shear stress. Chen et al. [6] have shown that the flow around the pin occurs in a "one by one", or wiping, flow pattern. Dynamic recrystallization (DXZ) [7], grain growth [8], and resolution and re-precipitation of phases [9] occur within this DXZ region. Further away, a "critical isotherm" exists [3] where the state of stress is less than the flow stress of the material, and this defines the boundary of the thermal-mechanically affected zone (TMAZ). Within the TMAZ, plastic deformation, grain growth and precipitate coarsening may occur without significant recrystallization [10]. The heat-affected zone (HAZ) outside the TMAZ experiences elastic deformation [4] and thermally induced microstructural changes [11] typical of that seen in fusion weld HAZ. The flow of material through these zones is highly cyclical with wiping pattern and force fluctuation frequency a function of pin tool design, material flow stress, and temperature-, strain- and process parameter-induced strain rates [12].

E-mail: william.arbegast@sdsmt.edu

1359-6462/$ - see front matter © 2007 Acta Materialia Inc. Published by Elsevier Ltd. All rights reserved.
doi:10.1016/j.scriptamat.2007.10.031

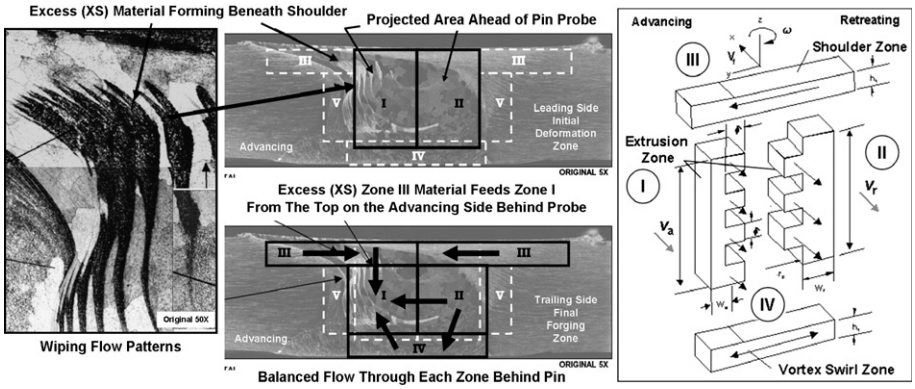

Figure 1. Flow-partitioned deformation zone geometries forming within the extrusion zone [3].

The complex interactions of the pin tool design, material properties and process parameter effects on defect formation are important. To date, existing CFD flow models do not address defect formation. In this paper, a simple partitioned mass balance flow model is proposed which relates defect formation to the volume (mass) and direction of material flowing through specific, and distinct, flow zones within the FSW.

2. Relationship of flow zone formation to defect formation

Several characteristic defects (Fig. 2) are seen to occur within the FSW and are identified as either flow or geometric related [13]. The geometric lack of penetration/fusion defect occurs due to improper pin tool penetration depth or improper seam tracking. The flow-related defects occur outside the acceptable processing window with parameters that are considered either too hot or too cold. Under hot processing with stick conditions, excessive material flow results with flash formation, surface galling and nugget collapse. Under cold processing with slip conditions, insufficient flowing material results in surface lack of fill, wormhole, or lack of consolidation defects on the advancing side (listed in terms of increasing forge force). It is postulated that the optimum processing conditions to prevent flow-related defects occur at a temperature where stick–slip wiping flow occurs and material flowing from the region ahead of the pin tool is exactly balanced with that flowing back into the vacated region behind the tool.

Advancing (Zone I) and a retreating (Zone II) deformation zone geometries form around the pin probe with different volume, velocity and flow directions. Material passing through Zone II moves downward and around the probe and converges with the material in Zone I. Material passing through Zone II may move far enough downward to enter Zone IV beneath the probe tip and again rise to merge with the materials within Zone I. The Zone III material originating on the retreating side is dragged across the top toward the advancing side. This retreating side Zone III material is ''interleaved'' with the Zone III material originating on the advancing side and forced (pumped) downward to fill Zone I from the top. Excess flow of Zone III material into Zone I results in nugget collapse. Loss of material from Zones II, III or IV due to flash, a raised crown, sheet lifting or sheet separation results in insufficient material entering Zone I and a surface lack of fill, wormhole or lack of consolidation (microvoid/scalloping) volumetric defect

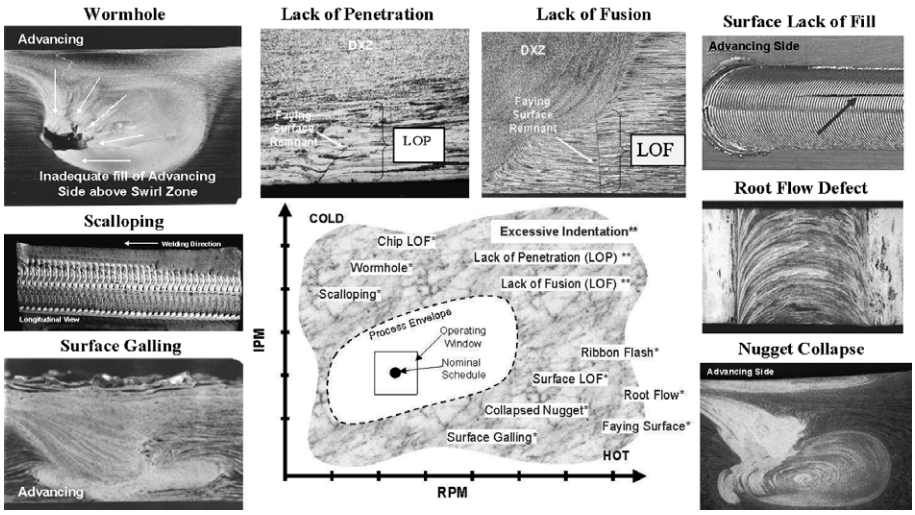

Figure 2. Characteristic defect types in friction stir welds [13].

depending on the level of forging force. Inadequate depth of material flowing in Zone IV beneath the probe tip contributes to the lack of penetration defect while excessive material flowing into Zone IV results in the root flow (over-penetration) defect. A fifth flow zone (Zone V) has been observed under very hot conditions where the downward flow is reversed upwards into a recirculation pattern. In lap joints, this contributes to sheet thinning, or hooking, defect formation.

3. Processing parameter effects on flow zone formation

Debate exists about whether material passes around the pin on both the advancing side (Zone I) and retreating sides (Zone II), or only around the retreating side. In this model (which assumes a typical low-angle convex shoulder, cylindrical, left-hand, fine-thread pitch pin tool under clockwise rotation) both cases are allowed (Fig. 3). Case (a) assumes a zero pin rotation speed ($\omega = 0$) and a positive forward travel speed ($v > 0$). The volume of material processed in the shoulder zone equals zero ($V^{S} = 0$) with the volume passing through the advancing side equal to the volume passing around the retreating side ($V^{R} = V^{A}$). This material must flow equally through a non-zero extrusion zone width (W) on the advancing and retreating sides ($W^{A} = W^{R}$). The width of these extrusion zones on each side are governed by the temperature field, constitutive properties, strain rate conditions and pin tool geometry as suggested by Colegrove. The overall height of the pin probe is less than the material thickness and some material passes beneath the probe tip (Zone IV) from the front to the back ($V^{P} > 0$). Metallurgical confirmation of these trends in flow zone formation based on optically observable flow pattern features, dissimilar alloy FSW and forced grain growth studies in aluminum alloy FSW are shown in Figure 4.

In case (b), the rotation speed increases slightly ($\omega_1 > \omega_0$) while the travel speed remains constant ($v_1 = v_0$). Slip conditions predominate. Material begins to rotate beneath the shoulder ($V_1^{S} > 0$). The volume passing around the pin probe on the retreating side is greater than the advancing side ($V_1^{R} > V_1^{A}$). The critical shear deformation boundary forms adjacent to the probe and a strain discontinuity occurs to define the width of the advancing (W_1^{A}) and retreating (W_1^{R}) side extrusion zones. (Note: In FSW of dissimilar alloys, the material constitutive properties may differ for each side.) This pin rotation also results in a greater volume of material passing around the probe tip ($V_1^{P} > V_0^{P}$) as evidenced by a greater depth of penetration.

In case (c), the rotation speed again increases ($\omega_2 \gg \omega_0$) with more heat generated beneath the shoulder with an increase in the flowing volume ($V_2^{S} > V_1^{S}$). Likewise, the higher rotation speed results in more material passing around the retreating side than the advancing side ($V_2^{R} \gg V_2^{A}$). Stick–slip conditions occur. The higher local temperatures result in smaller critical shear extrusion zone widths ($W_2^{R} < W_1^{R}$) and the addition of excess flowing material (V_{I}^{XS}, V_{II}^{XS}, $V^{XS} = V_{III}^{A\ XS} + V_{III}^{R\ XS}$, V_{IV}^{XS}) defined and bounded by the critical isotherm associated with each zone.

Case (d) represents excessively high rotation speeds ($\omega_3 \ggg \omega_0$) with the volume of material flowing through the shoulder ($V_3^{S} + V^{XS}$) much greater than through the other zones ($V_3^{A} \lll V_3^{R} \ll V_3^{S} + V^{XS}$). Stick conditions predominate. This perturbates the interleaving of advancing and retreating side shoulder zone material with the excess (V^{XS}) diving downward to fill Zone I. The high temperatures form a localized shear discontinuity very close to the pin probe resulting in much smaller advancing (V_3^{A}) and retreating side (V_3^{R}) flow zones. The increased downward motion of the retreating side flow (V_3^{R}) causes an increase in the volume flowing beneath the pin tip ($V_3^{P} > V_2^{P}$).

4. Mass balance and flow partitioning model for defect formation

A critical total mass flux of material (M_T^{cr}) must move from the front leading-edge to the trailing-edge through the extrusion zone cross-sectional area per revolution to

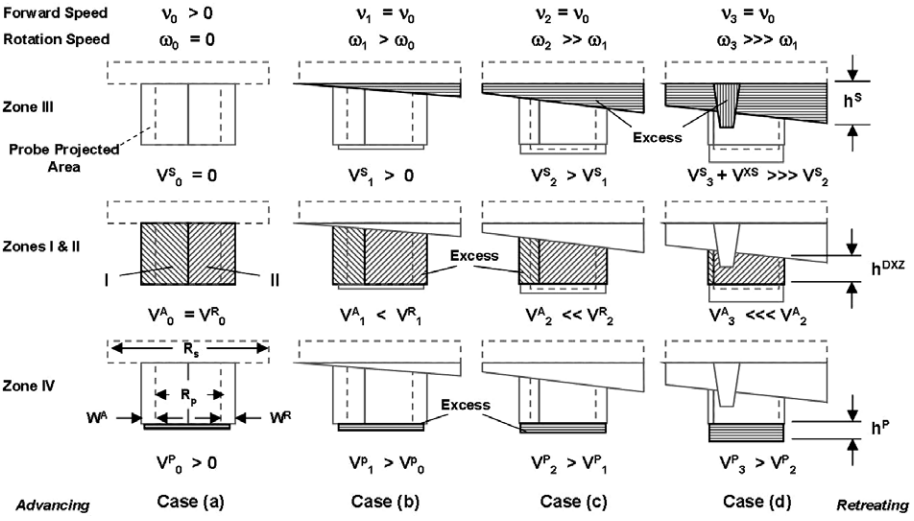

Figure 3. Processing parameter effects on deformation flow zone geometry at constant travel speed.

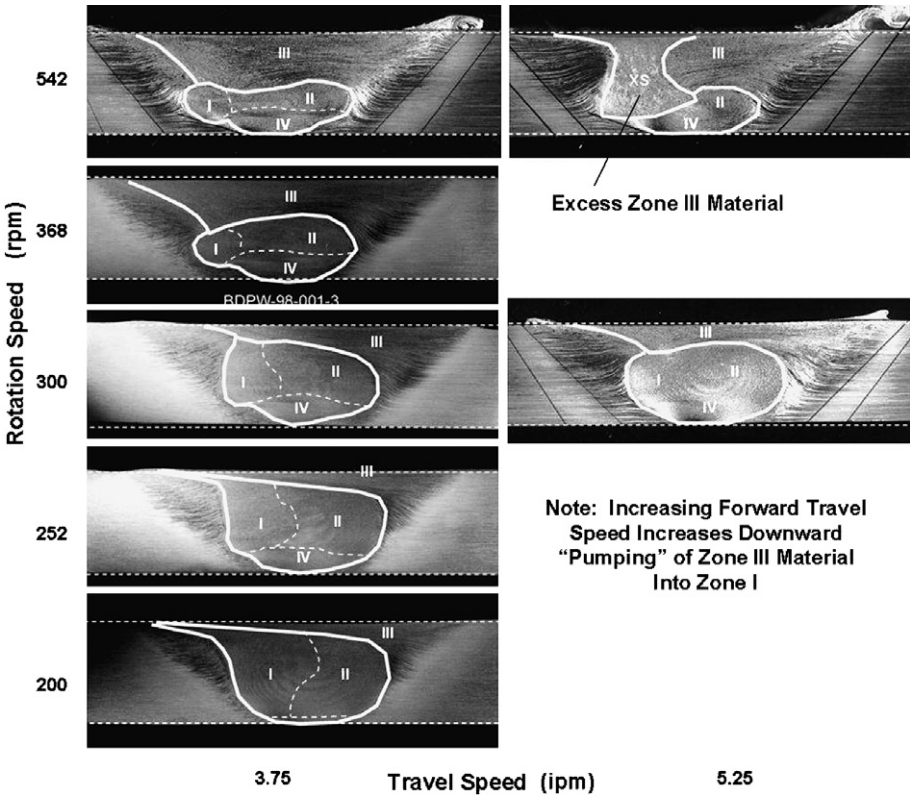

Figure 4. Effect of rotation speed and travel speed on flow partitioning and the volume of material flowing through the distinct zones formed during FSW of an aluminum alloy.

maintain mass balance and prevent volumetric (void) formation. Eq. (1) is proposed to equate this critical mass flux per revolution for typical fixed pin geometry in terms of the pin probe shape factor α (mm^{-1}), pin shoulder shape factor β (mm^{2}) and processing parameters $\phi = \omega/v$ (mm^{-1}) as originally defined in Ref. [3]

$$M_{\mathrm{T}}^{\mathrm{cr}} = \rho(\alpha \cdot \beta \cdot \phi^{2})^{-1}. \tag{1}$$

From the above, the total critical mass flux through the extrusion zone area can be represented by Eq. (2) where ρ_i is the density, v_i is the forward travel speed and ω_i is the rotation speed at each specific location (i) within the extrusion zone

$$M_{\mathrm{T}}^{\mathrm{cr}} = \sum \rho_i \left(\alpha \cdot \beta \cdot \left(\frac{\omega_i}{v_i} \right)^{2} \right)^{-1}. \tag{2}$$

$M_{\mathrm{T}}^{\mathrm{i}}$ is defined as the mass of the control volume entering the initial deformation zone (Eq. (3)), $M_{\mathrm{T}}^{\mathrm{e}}$ as the total mass processed within the extrusion zone (Eq. (4)), and $M_{\mathrm{T}}^{\mathrm{f}}$ as the total mass entering the final forging zone (Eq. (5)). Within the extrusion zone ($M_{\mathrm{T}}^{\mathrm{e}}$), excess material ($M_{\mathrm{T}}^{\mathrm{XS}}$) is added to the initial control volume ($M_{\mathrm{T}}^{\mathrm{i}}$). The amount of this excess material is determined by a boundary condition factor (Ψ_j) defined by the critical isotherm, flow stress and pressure distributions around the pin tool and beneath the shoulder (Fig. 5):

$$M_{\mathrm{T}}^{\mathrm{i}} = M_{\mathrm{I}}^{\mathrm{i}} + M_{\mathrm{II}}^{\mathrm{i}} + M_{\mathrm{III}}^{\mathrm{i}} + M_{\mathrm{IV}}^{\mathrm{i}} = \sum_{j=I}^{\mathrm{IV}} M_j^{\mathrm{i}}, \tag{3}$$

$$M_{\mathrm{T}}^{\mathrm{e}} = M_{\mathrm{T}}^{\mathrm{i}} + M_{\mathrm{T}}^{\mathrm{XS}} = \sum_{j=I}^{\mathrm{IV}} M_j^{\mathrm{i}} + \sum_{j=I}^{\mathrm{IV}} M_j^{\mathrm{XS}}, \tag{4}$$

$$M_{\mathrm{T}}^{\mathrm{f}} = M_{\mathrm{I}}^{\mathrm{f}} + M_{\mathrm{II}}^{\mathrm{f}} + M_{\mathrm{III}}^{\mathrm{f}} + M_{\mathrm{IV}}^{\mathrm{f}} = \sum_{j=I}^{\mathrm{IV}} M_j^{\mathrm{f}}. \tag{5}$$

For balanced flow and conservation of mass, $M_{\mathrm{T}}^{\mathrm{f}} = M_{\mathrm{T}}^{\mathrm{cr}}$. For unbalanced flow and volumetric defect formation $M_{\mathrm{T}}^{\mathrm{f}} < M_{\mathrm{T}}^{\mathrm{cr}}$ such that $M_{\mathrm{T}}^{\mathrm{f}} = M_{\mathrm{T}}^{\mathrm{e}} + M_{\mathrm{T}}^{\mathrm{wh}}$ where $M_{\mathrm{T}}^{\mathrm{wh}} > 0$ is the "wormhole mass deficiency" in the final forging zone. Eq. (6) defines this mass deficiency as the difference between the critical mass ($M_{\mathrm{T}}^{\mathrm{cr}}$), the initial control volume ($M_{\mathrm{T}}^{\mathrm{i}}$) and the excess material factor ($\Psi_j(\alpha, \beta, \phi^2)$) which defines the extra flowing material introduced within the extrusion zone. Eq. (7) defines a mass partitioning function (MPF) and is the forcing function which causes material to flow from one zone (j) into another zone (k) under the combined applied rotational, translational and forging forces (Θ_{jk}):

$$M_{\mathrm{T}}^{\mathrm{wh}} = M_{\mathrm{T}}^{\mathrm{cr}} - \sum_{j=I}^{\mathrm{IV}} M_j^{\mathrm{i}} - \sum_{j=I}^{\mathrm{IV}} \Psi_j(\alpha, \beta, \phi^2), \tag{6}$$

$$\mathrm{MPF} = \sum_{j,k=I}^{\mathrm{IV}} \Theta_{jk}(\alpha, \beta, \phi^2). \tag{7}$$

The wiping flow through each of the processing zones can be represented by a multi-body coupled dynamic system where the motion of one body affects the motion of an adjacent body. The position ($\bar{q}_{\mathrm{p}}$) and velocity ($\dot{\bar{q}}_{\mathrm{p}}$) state variables, mass matrix ([M]) and forcing function

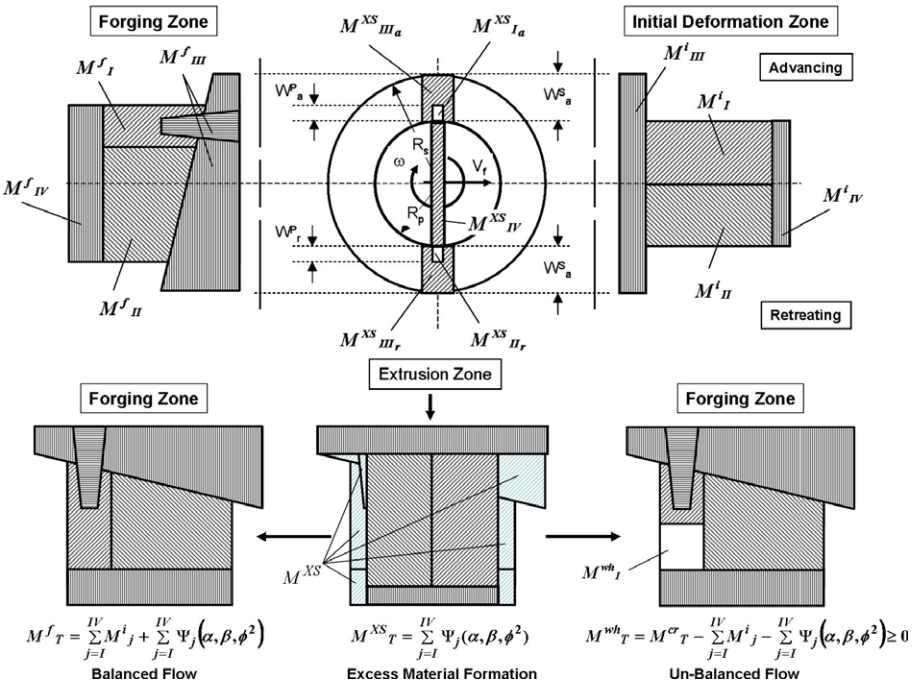

Figure 5. Schematic showing initial material entering FSW extrusion zone, formation of excess flowing material and formation of volumetric void from insufficient flow and fill of Zone I.

([MPF]) are expressed through the equations of motion: $[M]\cdot\ddot{\vec{q}} = [\mathrm{MPF}]$. The forcing function contains the instantaneous rotational, translational and forging forces at specific coordinate system locations and governs the material flow direction through each zone. The mass matrix includes the initial material flowing into, and the excess material formed within, each processing zone. From these, the following can be shown for balanced flow (Eq. (8)) and unbalanced flow (Eq. (9)):

$$\left(\sum_{j=I}^{\mathrm{IV}} M_j^{\mathrm{i}} + \sum_{j=I}^{\mathrm{IV}} \Psi_j(\alpha,\beta,\phi^2)\right)\cdot\ddot{\vec{q}}_{\mathrm{p}} = \sum_{j,k=I}^{\mathrm{IV}} \Theta_{jk}(\alpha,\beta,\phi^2), \quad (8)$$

$$\left(M_{\mathrm{T}}^{\mathrm{wh}} + \sum_{j=I}^{\mathrm{IV}} M_j^{\mathrm{i}} + \sum_{j=I}^{\mathrm{IV}} \Psi_j(\alpha,\beta,\phi^2)\right)\ddot{\vec{q}}_{\mathrm{p}} = \sum_{j,k=I}^{\mathrm{IV}} \Theta_{jk}(\alpha,\beta,\phi^2). \quad (9)$$

5. Summary

A flow-partitioned deformation zone model has been proposed to describe the conditions under which volumetric defects will, or will not, form during wiping flow in a FSW. The model assumes a critical mass of material ($M_{\mathrm{T}}^{\mathrm{cr}}$) necessary to maintain balanced flow and prevent volumetric wormhole formation. A mass deficiency factor ($M_{\mathrm{T}}^{\mathrm{wh}}$) is introduced to represent the volumetric defect. An excess material factor (Ψ) describes the flowing material added to the incoming control volume due to the temperature field, constitutive properties and strain rate conditions beneath the shoulder and around the pin. A flow partitioning function (Θ) is presented which describes the flow of material from one zone (j) into another (k) under the applied rotational, translational and forging forces. These are equated using the equations of motion for a multi-body dynamic system.

References

[1] W.J. Arbegast, Weld. J. 85 (3) (2006) 28–35.
[2] R.S. Mishra, Z.Y. Ma, Mater. Sci. Eng. 50 (2005) 1–78.
[3] W.J. Arbegast, Hot Deformation of Aluminum Alloys III, TMS, Warrendale, PA, 2003, pp. 313–327.
[4] P.A. Colegrove, H.R. Shercliff, R. Zettler, Sci. Technol. Weld. Join. 12 (4) (2007) 284.
[5] H. Schmidt, J. Hattel, Friction Stir Welding and Processing III, TMS, Warrendale, PA, 2005, p. 205.
[6] Z.W. Chen, T. Pasang, Y. Qi, R. Perris, In: 6th International FSW Symposium, TWI Ltd., Cambridge, 2006.
[7] R.W. Fonda, J. Wert, A. Reynolds, W. Tang, Sci. Technol. Weld. Join. 12 (4) (2007) 304.
[8] Y.S. Sato, H. Watanabe, H. Kokawa, Sci. Technol. Weld. Join. 12 (4) (2007) 318.
[9] V. Dixit, R.S. Mishra, R.J. Lederich, R. Talwar, Sci. Technol. Weld. Join. 12 (4) (2007) 334.
[10] Z. Feng, X.L. Wang, S.A. David, P.S. Sklad, Sci. Technol. Weld. Join. 12 (4) (2007) 348.
[11] M.M. Attallah, C.L. Davis, M. Strangwood, Sci. Technol. Weld. Join. 12 (4) (2007) 361.
[12] W.J. Arbegast, Friction Stir Welding and Processing III, TMS, Warrendale, PA, 2005.
[13] W.J. Arbegast, Friction Stir Welding and Processing, ASM International, Materials Park, OH, 2007, ISBN-13 978-0-87170-840-3, (Chapter 13).